

Article

Interrogating the Role of Receptor-Mediated Mechanisms: Biological Fate of Peptide-functionalized Radiolabeled Gold Nanoparticles in Tumor Mice

Francisco Silva, Ajit Prakash Zambre, Maria Paula Cabral Campello,
Lurdes Gano, Isabel Rego Santos, Ana Maria Ferraria, Maria João Ferreira,
Amolak Singh, Anandhi Upendran, António Paulo, and Raghuraman Kannan

Bioconjugate Chem., **Just Accepted Manuscript** • DOI: 10.1021/acs.bioconjchem.6b00102 • Publication Date (Web): 22 Mar 2016

Downloaded from <http://pubs.acs.org> on March 25, 2016

Just Accepted

"Just Accepted" manuscripts have been peer-reviewed and accepted for publication. They are posted online prior to technical editing, formatting for publication and author proofing. The American Chemical Society provides "Just Accepted" as a free service to the research community to expedite the dissemination of scientific material as soon as possible after acceptance. "Just Accepted" manuscripts appear in full in PDF format accompanied by an HTML abstract. "Just Accepted" manuscripts have been fully peer reviewed, but should not be considered the official version of record. They are accessible to all readers and citable by the Digital Object Identifier (DOI®). "Just Accepted" is an optional service offered to authors. Therefore, the "Just Accepted" Web site may not include all articles that will be published in the journal. After a manuscript is technically edited and formatted, it will be removed from the "Just Accepted" Web site and published as an ASAP article. Note that technical editing may introduce minor changes to the manuscript text and/or graphics which could affect content, and all legal disclaimers and ethical guidelines that apply to the journal pertain. ACS cannot be held responsible for errors or consequences arising from the use of information contained in these "Just Accepted" manuscripts.



ACS Publications

Interrogating the Role of Receptor-Mediated Mechanisms: Biological Fate of Peptide-functionalized Radiolabeled Gold Nanoparticles in Tumor Mice

Francisco Silva^{†§}, Ajit Zambre^{‡§}, Maria Paula Cabral Campello^{*†}, Lurdes Gano[†], Isabel Santos[†], Ana Maria Ferraria[#], Maria João Ferreira[¶], Amolak Singh[‡], Anandhi Upendran[⊥], António Paulo^{*†} and Raghuraman Kannan^{*‡¶⊥}

[†]Centro de Ciências e Tecnologias e Nucleares, Instituto Superior Técnico, Universidade de Lisboa, [#]Centro de Química-Física Molecular, Instituto Superior Técnico, Universidade de Lisboa, Portugal, ^{*}Centro de Química Estrutural, Instituto Superior Técnico, Universidade de Lisboa, Portugal
Departments of [‡]Radiology, [⊥]MU-iCATS, [¶]BioEngineering, and [⊥]International Center for Nano/Micro Systems and Nanotechnology, University of Missouri, Missouri-65211, USA

Keywords: Peptide, GRP receptors, Gallium, gold nanoparticles, tumor.

Corresponding Authors: Raghuraman Kannan, Department of Radiology, One Hospital Dr. Columbia, MO 65211. USA E-mail: kannanr@health.missouri.edu
António Paulo and Maria Paula Cabral Campello,
Centro de Ciências e Tecnologias e Nucleares, Instituto Superior Técnico, Universidade de Lisboa, Portugal E-mail: apaulo@ctn.tecnico.ulisboa.pt

[§]Contributed equally to this manuscript

Abstract

To get a better insight on the transport mechanism of peptide-conjugated nanoparticles to tumor, we performed *in vivo* biological studies of bombesin (BBN) peptide functionalized gold nanoparticles (AuNPs) in human prostate tumor bearing mice. Initially, we sought to compare AuNPs with thiol derivatives of acyclic and macrocyclic chelators of DTPA and DOTA types. The DTPA derivatives were unable to provide a stable coordination of ^{67}Ga and, therefore, the functionalization with the BBN analogs was pursued only for the DOTA-containing AuNPs. The DOTA-coated AuNPs were functionalized with BBN[7-14] using a unidentate cysteine group or a bidentate thioctic group to attach the peptide. AuNPs functionalized with thioctic-BBN displayed highest *in vitro* cellular internalization ($\approx 25\%$, 15 min) in GRP expressing cancer cells. However, these results fail to translate to *in vivo* tumor uptakes. Biodistribution studies following intravenous (IV) and intraperitoneal (IP) administration of nanoconjugates in tumor bearing mice indicated that the presence of BBN influences to some degree the biological profile of the nanoconstructs. For IV administration, the receptor-mediated pathway appears to be outweighed by EPR effect. By contrast, in IP administration, it is reasoned that GRPr-mediated mechanism plays a role in pancreas uptake.

INTRODUCTION

Targeting nanoparticles selectively to tumor site remains a significant challenge. To overcome this challenge, several research studies focused on understanding the transport mechanism of nanoparticles to tumor.¹⁻⁸ Two types of mechanism, passive and active targeting are reported in the literature to explain delivery of nanoparticles to tumor.⁹ Passive targeting is based on the leakiness characteristics of the tumor; whereas, active targeting is based on the receptors that are overexpressed on the tumor. Nanoparticles choose either one or both of these mechanisms to reach the tumor site. Previous studies demonstrate that numerous parameters influence the choice of mechanism for *in vivo* delivery of nanoparticles to tumor.^{4, 10-15} Several endogenous parameters including size, charge, and surface-bound ligand play significant roles in deciding the mechanism of delivery of nanoparticles.^{4, 10-15} In addition, exogenous factors such as reticuloendothelial system (RES) sequestration and bio-corona formation are also responsible in the transport mechanism of NPs to tumor.^{16, 17} With regard to passive targeting, Xia and coworkers have demonstrated that 30 nm gold cages performed better *in vivo* when compared with 55 nm nanocages.¹⁸ In sharp contrast, Chan and coworkers have shown that smaller size gold nanoparticles (20 nm) exhibit a lower degree of tumor accumulation than did 100 nm particles.^{19, 20} These studies further demonstrate that multiple factors in addition to size play role in deciding final *in vivo* destination of nanoparticles in passive targeting. A similar observation is noted in the case of active targeting. Several novel approaches were developed for directing the nanoparticles toward receptors that are over expressed on the surface of the tumor. A variety of biomolecules including antibodies, ScFv fragments, affibodies, peptides, aptamers, and carbohydrates have been attached to nanoparticles and their selective uptake in tumor studied.^{4-6, 8, 21-25} Even though these approaches are relatively successful, it is not yet clear that surface bound biomolecules have a convincing role in targeting the tumor. Pioneering work by Park and coworkers demonstrate

that antibody targeted liposomes have not shown any increase in tumor uptake when compared with the non-targeted liposomes.²⁶ Nevertheless, Davis and coworkers have demonstrated that targeted nanoparticles showed enhanced efficacy than the non-targeted analogue.²⁷ As noted above, the ground rules for developing a successful targeted nanoparticles are still emerging.

To obtain further insight on the role of surface bound biomolecules in targeted delivery, herein we have systematically studied the *in vivo* tumor targeting characteristics of radiolabeled gold nanoparticles (AuNPs) covalently conjugated with bombesin peptides. Bombesin (BBN) peptide recognizes Gastrin Releasing Peptide (GRP) receptors that are over expressed in a variety of human tumors including prostate, breast and lung cancer.²⁸⁻³¹ In this study, the *in vivo* tumor uptake of these AuNPs is studied in prostate tumor bearing mouse models using Ga-67 as radiolabel. ⁶⁷Ga is a γ -emitting radionuclide that presents physical properties suitable for *in vivo* imaging by Single Photon Emission Computed Tomography (SPECT); moreover, the congener ⁶⁸Ga is an emerging positron emitter with increasing clinical relevance, namely for tumor imaging by Positron Emission Tomography (PET).³² For radiolabeling, gallium-chelating ligands DTPA or DOTA were surface attached aiming at a fast and stable coordination of ⁶⁷Ga. Before proceeding with the functionalization of the nanoparticles surface with the targeting peptides, it has been investigated if each type of ligand was able to achieve the desired stable coordination of ⁶⁷Ga. To confirm that active targeting plays a crucial role, receptor-blocking studies were performed. We studied whether the route of administration, intravenous and intraperitoneal, plays any role in active targeting mechanism. Our previous studies were focused more on *in vitro* demonstration of nanoconjugates in recognizing receptors on the cell surface and peptide conjugated gold nanoparticles internalize primarily via receptor mediated endocytosis.^{2, 33} In addition, we have also shown that radioactive bombesin gold nanoconjugates (¹⁹⁸AuNPs) localize in pancreas and have poor uptake in tumor in mice models.¹ In the present study, we report the

following results: (i) design, synthesis, and characterization of ^{67}Ga -labeled targeted AuNPs; (ii) understanding the *in vitro* stability, GRP receptor recognition and internalization efficacy of targeted AuNPs in human cancer cells; (iii) measuring the quantitative biodistribution of nanoparticles in tumor bearing mice models; (iv) comparing uptake of targeted nanoparticles in tumor mice by blocking receptors; and (v) evaluating the route of administration of nanoparticles for optimal tumor uptake.

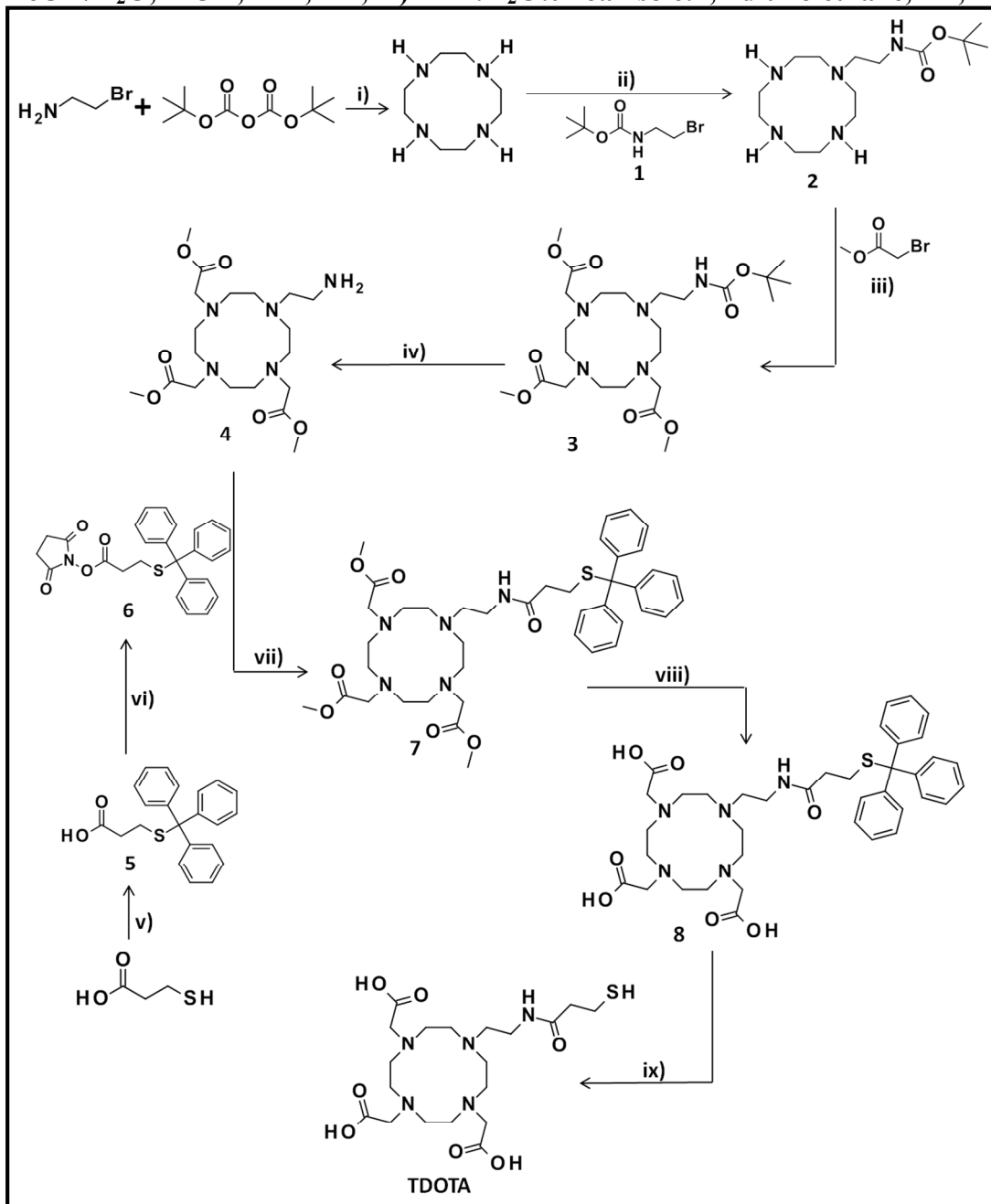
RESULTS AND DISCUSSION

It is important to design a robust and tunable nanoconstruct to effectively study the mechanism of tumor uptake in mice models. We have set out to obtain a library of BBN targeted ^{67}Ga -labeled nanoparticles of general formula $[\text{AuNP}(\text{L})(\text{R})]$, where L represents a polyamino carboxylic chelator and R can be a BBN derivative. These nanoconstructs would contain three important components: (i) *Component 1 (AuNPs)*: the nanoparticle core is comprised of rigid small core (3 - 5 nm) sized gold nanoparticles (AuNPs). The variation in core size was minimized throughout study. Several investigations have demonstrated that AuNPs are non-toxic, non-immunogenic, and are ideally suited for our study; (ii) *Component 2 (L)*: We investigated both DTPA and DOTA as ligands (L) for irreversibly chelating radiolabeled- ^{67}Ga and surface anchored to AuNPs. L contains both 'SH' group and amino carboxylates for attaching with AuNP and to chelate ^{67}Ga respectively. The radiolabeling method was chosen for performing quantitative *in vivo* biodistribution studies, since the measurement of radioactivity is a much more reliable method than the elemental analysis of gold (e.g. by fAAS, ICP or NAA). However, it is important to ensure irreversible attachment of the radionuclide to the surface of nanoparticle; and (iii) *Component 3 (BBN)*: the targeting molecule chosen for the study is a receptor-avid peptide, a bombesin derivative. Our rationale for choosing BBN is as follows: GRP receptors (called bombesin type 2 (BB_2) receptor) have high affinity for its natural ligand, bombesin (BBN).

Several clinical studies have shown that BBN analogues have superior targeting characteristics.³⁴⁻

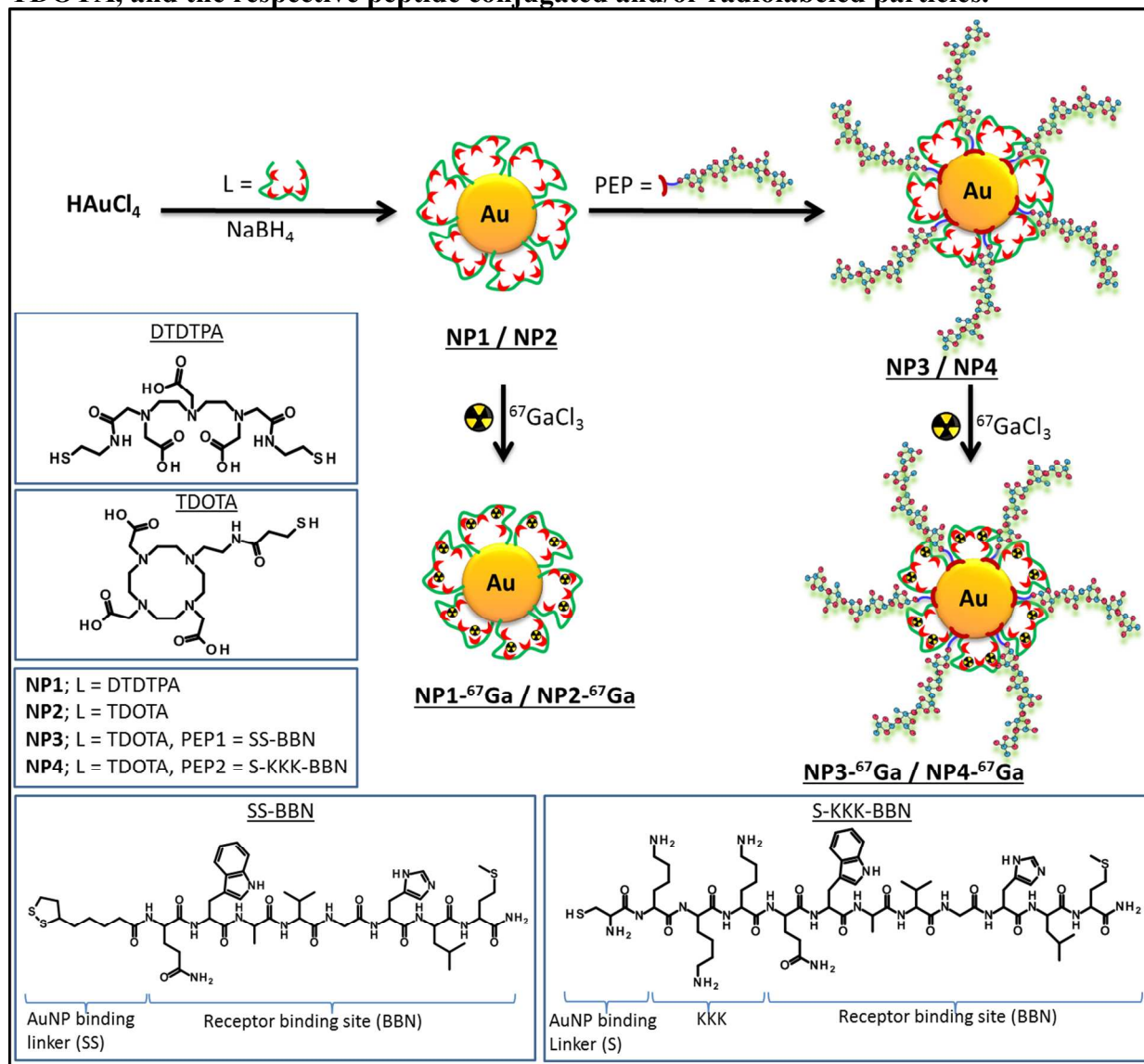
36

Scheme 1. Synthesis of TDOTA: i) MeOH, 24 h, RT; ii) Toluene, 24 h, reflux; iii) CH₃CN, Na₂CO₃, 8 h, 70 °C; iv) TFA/CH₂Cl₂, 2 h, RT; v) THF, Ph₃CSH, NaH, 30 min, RT; vi) CH₂Cl₂, NHS, EDC, DIPEA, 24 h, RT; vii) DMF/CH₂Cl₂, DIPEA, 24 h, RT; viii) THF/MeOH/H₂O, LiOH, 24 h, RT; ix) TFA:H₂O:thioanisole:1,2-dithiolethane, 2 h, RT.



The ligand framework – DTPA or DOTA – was attached on the surface of the nanoparticle by a stable thiol bond. Such proximity between ligand and nanoparticle provide rigidity and enhanced stability to the final construct. Several research studies have shown that both DTPA and DOTA are excellent chelating ligands for stabilizing Ga-67 in both molecular or nanosized frameworks.³⁷⁻⁴⁰ As such, both DTPA and DOTA ligands lack chemical functionality to directly attach with gold atoms. Hence, we devised synthetic strategies to incorporate thiol groups in the ligand structure being aware that the modification of these polyamine chelators (L) can influence the *in vivo* stability of ⁶⁷Ga-L that directly depends on the coordination saturation and *trans*-chelation with transferrin. We have focused on the already described thiolated DTPA derivative 2-[bis[2-[carboxymethyl-[2-oxo-2-(2-sulfanylethylamino)ethyl]amino]ethyl]amino]acetic acid (**DTDTPA**) and on a new thiolated DOTA derivative. This new DOTA derivative, trimethyl 2,2',2''-(10-2(3-(tritylthio)propamido)ethyl)-1,4,7,10-tetraazacyclododecane-1,4,7-trityl)triacetate (**TDOTA**), relied on the introduction of a single 2-ethylamine group in the cyclen framework, for further coupling to a thiolated pendant arm (**Scheme 1**). The synthesis of **TDOTA** started with the N-alkylation of cyclen by reaction with tert-butyl N-(2-bromoethyl) carbamate (**1**). The resulting monoalkylated cyclen derivative (**2**), containing a BOC protected pendant arm, was treated with methyl 2-bromoacetate to afford **3**. Then, removal of the BOC protecting group from **3** with TFA gave compound **4** displaying a terminal amino function for coupling of 3-mercaptopropionic acid. Treatment of **4** with a NHS activated ester of 3-mercaptopropionic acid (**6**), having the terminal thiol protected with a trityl group, yielded the amide derivative **7**. Basic hydrolysis of the methyl ester functions of **7** followed by acid deprotection of the trityl protecting groups led to the desired final compound.

Scheme 2. Synthesis of the non-targeted nanoconstructs stabilized with DTDTPA or TDOTA, and the respective peptide conjugated and/or radiolabeled particles.



Synthesis of targeted and non-targeted nanoconstructs

For synthesizing the nanoconstructs, we developed a step-wise ligand/peptide incorporation methodology. In the first step, the ligand framework was attached to the surface of AuNPs using the thiol groups of the modified DOTA or DTDTPA. Previously developed procedure was used to attach the DTPA derivative (**DTDTPA**) onto the surface of AuNPs, which led to the **AuNP-DTDTPA (NP1)** nanoconstructs (**Scheme 2**).⁴¹⁻⁴⁴ Details of the synthetic procedure are presented

in the experimental section (see Supplementary Information). Similar to **NP1**, the strategy for the synthesis of the AuNPs stabilized with **TDOTA** was also based on the modified procedure of Brust et al.⁴⁵ As shown in **Scheme 2**, this involved the reduction of $\text{HAuCl}_4 \cdot 3\text{H}_2\text{O}$ with NaBH_4 in the presence of **TDOTA** using a molar ratio of 1:2.5 (Au:TDOTA) that resulted in the formation of a dark brown solution of DOTA stabilized gold nanoconstructs designated as **AuNP-TDOTA (NP2)**. AuNP-L (L = **DTDTPA** and **TDOTA**) were purified by centrifugation methods, washed and used for subsequent steps.

As a next step, we focused on synthesizing radiogallium conjugates of **NP1** and **NP2** by reacting the nanoconstructs with $^{67}\text{GaCl}_3$. We optimized the procedure by radiolabeling nanoconjugates at different pH and reaction times. In a typical reaction, **NP1** or **NP2** (11.4 μmol) was dissolved in acetate buffer at pH 7 and mixed with $^{67}\text{GaCl}_3$ (70-120 MBq) in 0.1 M HCl, the reaction mixture was left undisturbed at 50° C. Each reaction mixture was purified by ultra-filtration and the respective radiolabeled conjugate analyzed using Radio-TLC. Radio-TLC control provided a quantifiable data on the radiochemical yield and purity. The final ^{67}Ga -labeled nanoconstructs **NP1- ^{67}Ga** and **NP2- ^{67}Ga** were obtained with radiochemical yields of 86 and 88%, respectively, and with a radiochemical purity > 95%.

It is important to study the stability of the radiolabelled **NP- ^{67}Ga** conjugates in the presence of biologically relevant media and apo-transferrin. Ga-67 attached to weakly stable chelate is susceptible for trans-chelation with apo-transferrin, resulting in leaching of gallium from the chelate. Thus, this test acts as an independent measure to evaluate the stability of the nanoconjugate. For the stability studies, **NP- ^{67}Ga** nanoconjugates were suspended in 0.1 M PBS, NaCl 0.9%, cell culture medium and apo-transferrin (3 mg/mL, in 10 mM NaHCO_3) and incubated at 37 °C. At different intervals of time, a small amount of solution was removed and analyzed using radio-TLC (up to 24 hours). The details are presented in a graph (**ESI-Figure 6**).

The ^{67}Ga -labelled nanoconstruct functionalized with **DTDTPA** (**NP1- ^{67}Ga**) showed poor stability in apo-transferrin when compared to the one functionalized with **TDOTA** (**NP2- ^{67}Ga**). In addition, **NP2- ^{67}Ga** has shown a moderate to high stability in all biological media, although, there is some decrease in the percentage of radiolabeled nanoconstruct for the shortest incubation times but for longer incubation times such percentage remained fairly constant. Due to the inability of **NP1** to provide a stable coordination of Ga-67, we did not use this nanoplatform for further functionalization with the BBN peptides. The observed instability would lead to unreliable data regarding the biological profile of the corresponding BBN-conjugated AuNPs when performing cellular (*in vitro*) and animal (*in vivo*) studies, due to a high probability that the radioactivity distribution would not reflect that of the nanoparticles.

After confirming that AuNP-TDOTA (**NP2**) nanoconstruct possess suitable coordinating properties to attach Ga-67, **NP2** was functionalized with BBN peptides. We used two different BBN analogs in our study (SS-BBN, S-KKK-BBN; **Scheme 2**). In both the analogs the amino acid sequence BBN[7-14] remain unaltered; however, the functional group that allows for the binding to the gold surface is altered. In SS-BBN, the thioctic acid group ligate with nanoparticles, while for S-KKK-BBN, it was through cysteine -SH. We hypothesized that cysteine would allow increased loading of peptide on AuNPs. The possibility of increasing the peptide loading was expected to enhance the targeting ability of the BBN-containing AuNPs.

We used a 1:2 ratio (w/w) of AuNP:BBN for functionalizing **NP2** (**Scheme 2**), both with SS-BBN and S-KKK-BBN, to obtain **NP3** and **NP4**, respectively. After reaction, the amount of unreacted BBN analogs was estimated using HPLC. The concentration of SS-BBN attached in **NP3** was 0.86 μmol (0.98 mg), while the amount of S-KKK-BBN attached in **NP4** was 0.17 μmol (0.24 mg) per mg of nanoparticle. As mentioned above, the conjugation of S-KKK-BBN to the AuNPs involves uniquely the formation of one Au-S bond and, therefore, the coupling of the

same number of peptide molecules involves less number of gold atoms if compared with SS-BBN. This is why one could expect that it should be possible to attach a high number of peptide molecules to the AuNPs in the case of S-KKK-BBN. However, the involvement of two sulfur atoms per molecule in the conjugation of SS-BBN to the AuNPs can lead to a more stable binding, which eventually justifies the higher payload that has been achieved in the case of this BBN derivative. The characterization details of these BBN-containing nanoconjugates and respective precursor AuNPs (UV-visible, TEM analysis, charge and hydrodynamic size distribution, nanoparticle tracking analysis, XPS, proton and HSQC NMR) are presented in supporting information (ESI-Figure 1 – ESI-Figure 5; Table 1; and ESI-Table 1).

Table 1. Physico-chemical characterization of nanoconjugates synthesized in the present study.

Nanoparticle*	UV-Vis (nm)	TEM (nm)	Hydrodynamic size (nm) (PDI)	Zeta-potential (mV)
NP1	520	2.28 ± 1.32	100.6 (0.111)	-80.7 ± 15.6
NP2	520	4.29 ± 1.60	20.6 (0.342)	-62.6 ± 18.6
NP3	520	4.79 ± 1.50	22.5 (0.420)	-60.5 ± 16.4
NP4	520	4.04 ± 1.52	47.35 (0.370)	-30.1 ± 16.8

*All measurements were performed by preparing the nanoparticle solution in DI water (≈ pH 6)

Nanoconstructs **NP3** and **NP4** were successfully radiolabeled with Ga-67 following the same procedure described previously for **NP2** (Table 2). The resulting nanoparticles, **NP3-⁶⁷Ga** and **NP4-⁶⁷Ga**, were obtained with radiochemical yields of 69% and 71%, respectively, and with a radiochemical purity > 95%.

The stability of **NP3-⁶⁷Ga** and **NP4-⁶⁷Ga** was studied in the presence of relevant biological media and apo-transferrin (ESI-Figure 6). Overall, **NP3** and **NP4** maintain a moderate to high stability as seen previously for their precursor **NP2**. However, among these radiolabelled DOTA

conjugated **NP2-NP4**, **NP4** showed least stability. Nevertheless, more than 60% of **NP4-⁶⁷Ga** did not release ⁶⁷Ga even after 24 h of incubation with cell medium. It is possible that the positively charged amino acids (lysine) present in peptide backbone of **NP4** repel with positive charged gallium ions in the close proximity resulting in their leaching. Gallium ions farther from lysine residues are stably coordinated and stay intact with no release during the study period.

Table 2. Reaction conditions for the ⁶⁷Ga-labelling of nanoconjugates and respective radiochemical yields.

Nanoparticle	Temperature (°C)	Reaction time (min)	Radiochemical yield (%)
NP1-⁶⁷Ga	50	15	86
NP2-⁶⁷Ga	50	30	89
NP3-⁶⁷Ga	50	30	69
NP4-⁶⁷Ga	50	30	71

Receptor affinity and cellular uptake of **NP3** and **NP4**

We used competitive binding assay to estimate the specificity of BBN conjugated nanoconstructs to GRP receptors overexpressed on the surface of cancer cells. In this assay, the ability of the nanoparticles to displace radioiodinated specific binding ligand was estimated. We used ¹²⁵I-Tyr₄-BBN as radioligand to assess the affinity of **NP(2-4)** in human prostate cancer cells (PC3). (**Figure 1**). As expected, **NP3** and **NP4** display a significant affinity towards GRP with IC₅₀ values of 0.045 ± 0.003 and 0.160 ± 0.027 µg/mL, respectively. In a similar fashion, **NP2** showed no affinity for GRP receptors. Among all the nanoconjugates, **NP3** has a lower IC₅₀ and it can be attributed to the increased number of BBN peptide present in this construct.

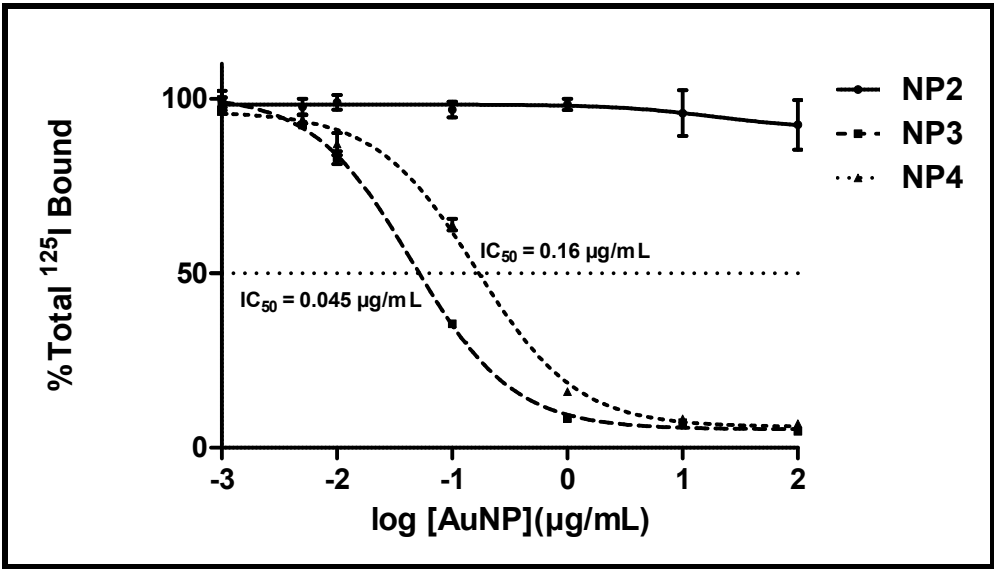


Figure 1. Representative binding affinity (mean \pm SD, $n=4$) of nanoconjugates **NP2**, **NP3** and **NP4** in PC-3 cells by competitive assays with ^{125}I -Tyr₄-BBN.

One of the crucial experiments to measure the specificity of radiolabeled nanoconjugates toward GRP receptors is to understand the internalization pattern. We performed receptor uptake studies in GRPr-positive human prostate cancer PC3 cells, by exposing the cells to a solution of the radiolabeled NPs (**NP(2-4)-⁶⁷Ga**) in cell culture medium and incubation at 37 °C for different intervals of time (**Figure 2**). The internalization observed for **NP2** and **NP4** showed a similar profile with a slow uptake reflected from the increase in radioactivity that reaches relatively low plateau values (< 2%). By contrast, **NP3-⁶⁷Ga** has shown a very high and rapid internalization into the cells with almost 25% internalization after 15 min of incubation; thereafter, there is a slow decrease in the uptake of radioactivity suggesting the release of the Ga ions from the cells. As stated before, the peptide load of **NP3** is roughly five-fold higher than **NP4**, which is certainly related with the trend observed for the cellular internalization as well for the binding affinities of the nanoconstructs towards GRPr in PC3 cells. Altogether, these findings indicated that the internalization of **NP3-⁶⁷Ga** should involve a receptor-mediated process. To further confirm that **NP3-⁶⁷Ga** is retained within PC3 cells, we investigated the efflux of radioactivity from the cell.

Typically, **NP3-⁶⁷Ga** was incubated in PC3 cells for 15 minutes, and the unbound nanoconjugates were washed. The radioactivity retained by the cells was measured. Then, the medium was replaced with culture medium without any radioactive compound and the radioactivity release was monitored at different intervals of time by washing and measuring the radioactivity associated with the cells again. A fast washout of the radioactivity has been observed during the first 2 h. However, thereafter, the efflux rate significantly decreases and the activity present in the cells remains essentially constant after 4 h of incubation, reaching roughly 40% of the initial radioactivity (ESI- **Figure 8**). Therefore, one can consider that the PC3 cells retained a reasonable amount of **NP3-⁶⁷Ga**, which was an encouraging result to further study the targeting ability of these AuNPs in GRP receptor positive tumors.

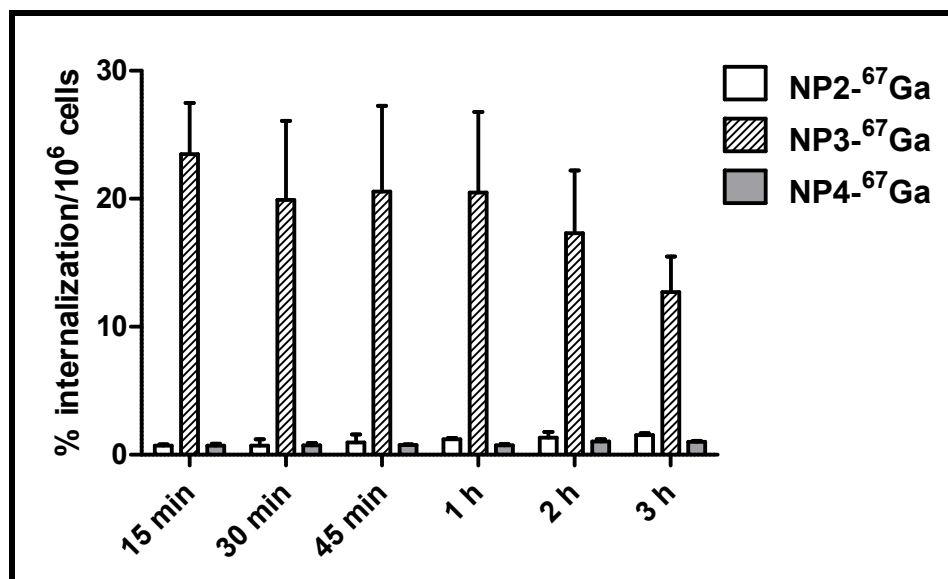


Figure 2. Cellular uptake (mean \pm SD, $n=4$) of **NP2-⁶⁷Ga**, **NP3-⁶⁷Ga** and **NP4-⁶⁷Ga** in PC3 cells, after incubation at 37 °C at different intervals of time. Internalization is expressed as the percentage of the applied radioactivity internalized by the cells.

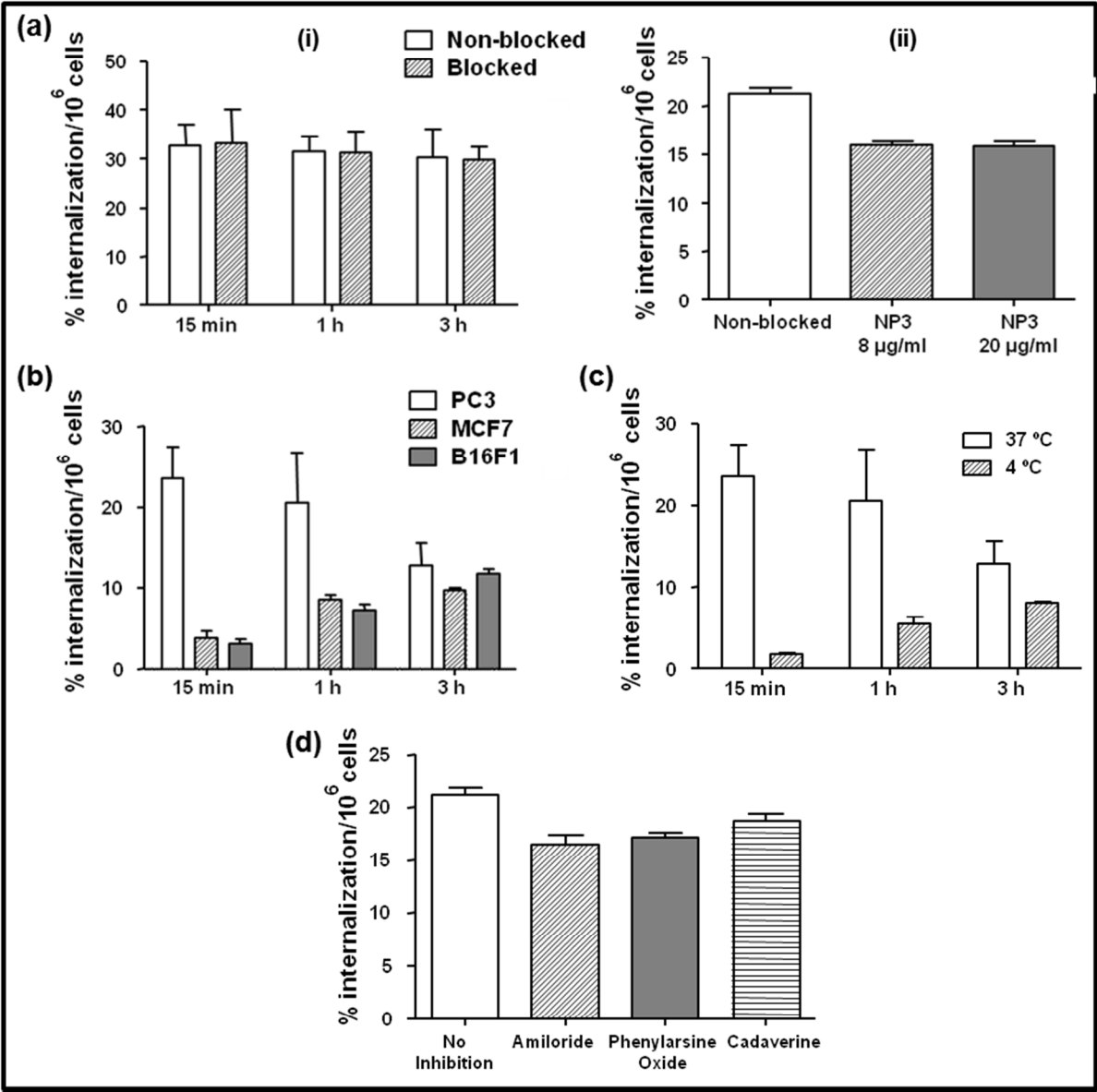


Figure 3. (a) Cellular uptake (mean \pm SD, $n=4$) of NP3-⁶⁷Ga at 37 °C in PC3 cells in the presence and absence of i) BBN (1 μ M/well) and ii) cold NP3 (8 μ g/mL and 20 μ g/mL per well); (b) Comparative cellular uptake (mean \pm SD, $n=4$) for NP3-⁶⁷Ga at 37 °C in PC3, MCF7 and B16F1 cell lines; (c) Comparison of cellular uptake of NP3-⁶⁷Ga at 37 and 4°C in PC3 cells; (d) Cellular uptake of NP3-⁶⁷Ga in the presence of amiloride, phenylarsine and cadaverine at 37 °C in PC3 cells. Internalization is expressed as the percentage of the applied radioactivity internalized by the cells.

Mechanism of Cellular Internalization of NP4-⁶⁷Ga Conjugate

As the focus of this study is to understand whether peptide conjugated nanoparticles undergo active targeting mechanism, we have performed a very systematic study to evaluate the mechanism of uptake of NP3-⁶⁷Ga in GRPr expressing PC3 cells. Several studies described above demonstrate that NP3-⁶⁷Ga exhibit high stability, cellular internalization, and retention. Therefore, our mechanistic studies were performed utilizing only this conjugate. We performed four experiments using NP3-⁶⁷Ga: (i) evaluate the effect of internalization of NP3-⁶⁷Ga after blocking the receptors with free peptide or cold NP3; (ii) compare the internalization of NP3-⁶⁷Ga in GRP receptor positive (PC3) and GRP receptor negative cells lines (human breast cancer MCF7 and mouse melanoma B16F1 cell lines); (iii) evaluate the energy dependence of the NP3-⁶⁷Ga in internalization; and (iv) evaluate the effect of internalization of NP3-⁶⁷Ga in the presence of cellular pathway blockers. *First*, GRP receptors on PC3 cells were blocked using free BBN and subsequently incubated with NP3-⁶⁷Ga. Thereafter, the amount of nanoparticles internalized at different time intervals was quantified (**Figure 3a(i)**). These studies showed that there is no significant difference in the amount of internalized radioactivity between the blocked and the non-blocked cells. The presence of BBN on the surface of the AuNPs clearly influences its internalization into the cells, but apparently the process involved is not mediated merely by the specific interaction with GRPr, as indicated by the inability of cold free BBN peptide to inhibit the uptake. It was hypothesized that the moderately large hydrodynamic size of NP3 (22.5 nm (PDI = 0.420)) could contribute for an easier saturation of the GRPr receptors in the cell membrane. As invoked by other authors, due to their size, a single nanoparticle can block the access to several receptor molecules, even without being involved in direct and specific interactions with such molecules.⁴⁶ On the flip side, a single NP3 having several copies of the bioactive peptide can specifically interact with more than one GRP receptor, leading to a strong

binding as found often for multimerized constructs, due to the so-called concept of avidity.⁴⁷ For all these reasons, monomeric BBN can be a less effective competitor in the GRP binding of **NP3-⁶⁷Ga** if compared with the cold **NP3** itself. Therefore, blockade experiments using increasing concentrations of cold **NP3** were performed (**Figure 3a (ii)**). No significant decrease of the amount of internalized radioactivity was observed, even using a 5-fold greater concentration of **NP3**, compared to the concentration of the radiolabeled AuNPs. It should also be taken into account that due to the low amount of ⁶⁷Ga present in the radiolabeling mixture ($< 4.7 \times 10^{-9}$ mmol) it is common to have non-radiolabeled AuNPs in the final **NP3-⁶⁷Ga** solution. These non-radiolabeled AuNPs will compete for the binding with GRP receptor. So far, the separation of the radiolabeled AuNPs from the non-radiolabeled ones was not possible with the available methodologies. In summary, blocking the GRP receptors on the surface does not affect internalization of **NP3-⁶⁷Ga** in PC3 cells. *Second*, internalization ability of **NP3-⁶⁷Ga** was investigated in both GRP receptor positive (PC3) and negative cell lines (human breast cancer MCF7 and mouse melanoma B16F1). It is observed that the initial rate of internalization is significant for the GRP positive PC3 cells (with $> 20\%$ of internalization observed), whereas in the GRP receptor negative cell lines less than 5% of internalization was observed at 15 min incubation. Moreover, there is a slow decrease in radioactivity from PC3 cells upon increasing incubation time, while a reverse trend (i.e.) a steady increase of internalization with the time of incubation was observed for the MCF7 and B16F1 cell lines. These results are indicative that the presence of GRPr influences the cellular uptake of the nanoparticles, taking into account the much faster internalization observed for the PC3 cells (**Figure 3b**). Altogether, these results prompt us to presume that the cellular internalization of **NP3-⁶⁷Ga** in PC3 cells is fairly mediated by the GRP receptors. *Third*, in order to gain more insight into the involvement of different energy dependent pathways in the internalization of **NP3-⁶⁷Ga** in PC3 cells, cellular uptake was

monitored at two different temperature conditions. The uptake of **NP3-⁶⁷Ga** in PC3 cells at 4 °C is less than at 37 °C; these results confirm that its cellular uptake involves energy dependent mechanisms, like phagocytic and endocytic pathways (**Figure 3c**). Similar results are observed in our previous study on BBN conjugated gold nanocages; these cages showed decreased cellular uptake at 4 °C in GRP expressing cancer cells.³³

Fourth, to investigate if the cellular internalization pathway is dependent on receptor-mediated endocytosis, cellular uptake was monitored in the presence of inhibitors of different cellular transport processes such as amiloride, phenylarsine oxide or cadaverine (endocytosis or phagocytosis inhibitors). These inhibitors decreased the cellular uptake of **NP3-⁶⁷Ga** up to 20% in PC3 cells (**Figure 3d**). Amiloride is a Na⁺/H⁺ channel inhibitor that is known to block macropinocytosis and phagocytosis pathways that correspond to non-receptor mediated pathways. Phenylarsine oxide or cadaverine, are both clathrin-mediated endocytosis (CME) inhibitors. In general, receptor based internalization of molecules involves clathrin machinery.⁴⁸ These results indicate that the uptake of **NP3-⁶⁷Ga** occurs most probably via active phagocytic and endocytic pathways, which in the latter case might involve the internalization of GRPr. Recently, we have shown that the uptake in PC3 cells of BBN-containing gold nanocages is mediated by CME, and confirmed the formation of characteristic clathrin coated pits with lysosomal release of the nanocages.³³ For **NP3-⁶⁷Ga**, the cellular uptake mechanistic study was not so detailed, and other internalization possibilities include other endocytic transport processes, namely caveolae (lipid transport) or alternative pathways need to be investigated. As proposed by other authors, the involvement of these alternative pathways may result from the aggregation of the individual nanoparticles, since clathrin mediation is size dependent.^{33, 49, 50} In fact, it is considered that nanoparticles can utilize CME to internalize the cells when their dynamical-aggregates are not superior to a 300 nm size limit.³³ As the hydrodynamic size of **NP3** was 22.5

nm (PDI = 0.420), it is conceivable that the internalization of NP3-⁶⁷Ga will occur through CME, with involvement of GRP, only when these AuNPs present themselves to the cell surface as individual “monomeric” nanoparticles.

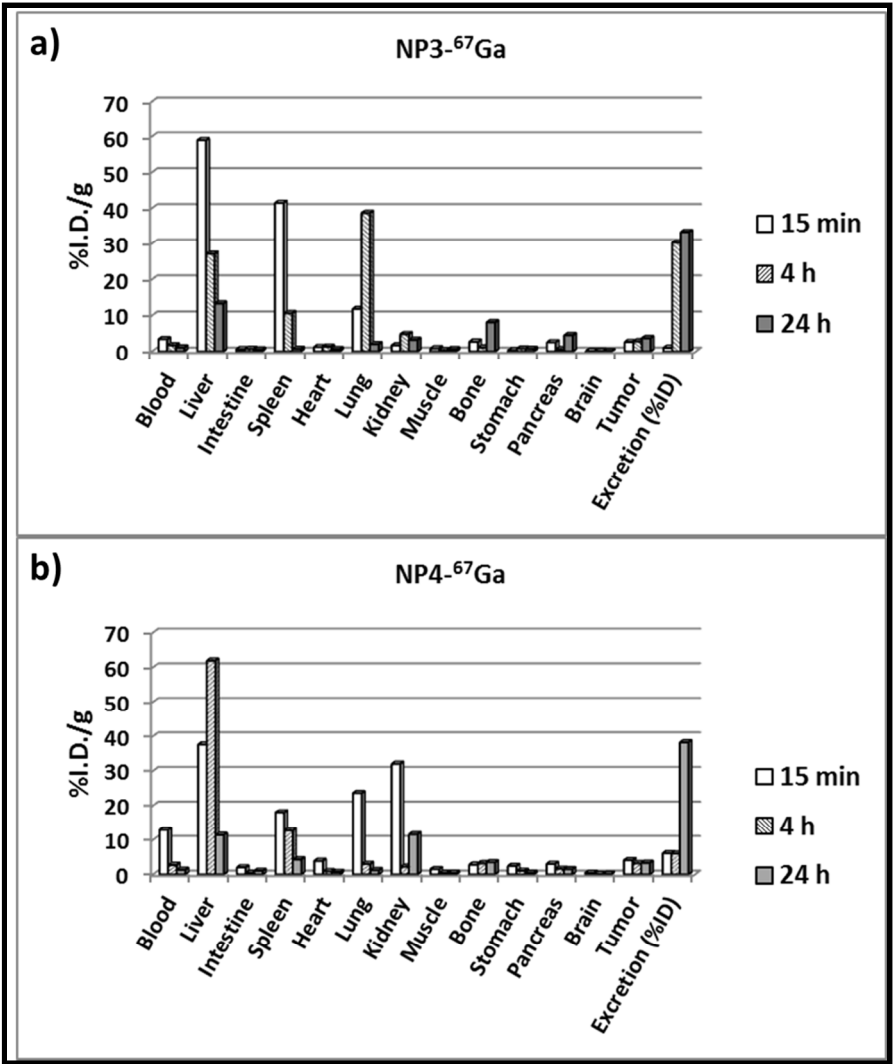


Figure 4. Biodistribution of (a) NP3-⁶⁷Ga and (b) NP4-⁶⁷Ga in tumor and organs in BALB/c nude mice bearing human prostate PC3 xenografts, injected intravenously via tail vein injection. Data are expressed as percentages of injected activity per gram of tissue (%ID/g), except for the GI tract, which is expressed as percentages of injected activity per organ. Error bars represent the mean ± standard deviation (n=3).

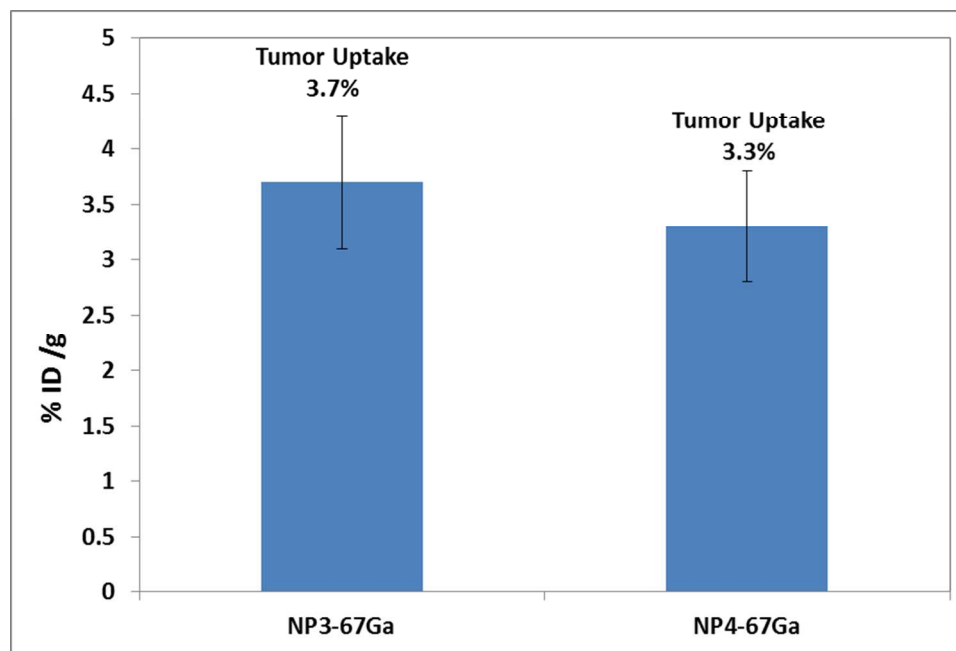


Figure 5. Comparison of tumor uptake of the BBN-containing radiolabelled nanoconstructs at 24 hrs post injection time point.

In vivo Studies

It is important to understand the biodistribution of nanoconjugates in tumor bearing mice before initiating mechanistic studies. Previous studies demonstrate that the nanoparticles preferentially accumulate in RES organs –liver and spleen. For example, Ga-67 labeled dextran-coated iron oxide showed 75% of ID accumulated in liver and spleen after 15 minutes post injection.⁴⁰ Our previous investigation showed that gum Arabic coated radioactive gold nanoparticle accumulates in liver and spleen.⁵¹ Of interest to the present study, we have demonstrated that gold nanoparticle-bombesin conjugates accumulate more than 50% ID/g in liver and spleen.¹ If the size of the nanoparticles is large, accumulation in lungs also predominate; however, smaller sized particles excrete via urine.⁵² As noted in previous sections, size alone does not dictate the fate and distribution of nanoparticles *in vivo*. Other factors such as charge, surface coating, zeta potential, and protein corona around nanoparticles play crucial roles in their accumulation and excretion. In

addition to the above, radiolabeled conjugates should establish *in vivo* structural integrity for effective uptake. Poor stability leads to release of radiolabel from conjugate resulting in diminished uptake in target organs, thus would draw wrong conclusions. Liu and coworkers have shown that Cu-64 alloyed gold nanoparticles showed uptake in spleen, instead of liver, due to release of the radiolabel and formation of smaller size particles.⁵³ Smaller sized radiolabeled particles were filtered by spleen and they used biodistribution data as a tool to establish the *in vivo* stability. In the present study, the structural integrity of the nanoconjugate was evaluated by measuring the uptake of radioactivity in RES and other non-target organs. Particularly, we investigated the biodistribution and tumor uptake of NP3-⁶⁷Ga and NP4-⁶⁷Ga (Figure 4 and 5; ESI-Table 2).

One of the important factors that represent the *in vivo* integrity of the nanoparticle is their uptake in RES organs. In general, most nanoconjugates show very high uptake in these organs and, therefore, it may serve as an independent parameter to evaluate their *in vivo* stability. For both ⁶⁷Ga labeled AuNPs reported herein (NP3-⁶⁷Ga and NP4-⁶⁷Ga), the general trend of the RES uptake remains similar for different time points, and the additional data are presented in the supporting information. At 4 hours post-injection time point, NP3-⁶⁷Ga showed the lowest uptake in liver and spleen (27.1 and 10.6% ID/g) when compared with NP4-⁶⁷Ga (61.9 and 12.7 %ID/g). A recent study with Ga-68 labeled NOTA ligand conjugated to hydrophilic bombesin showed less than 5% ID/g uptake in liver and spleen.⁵⁴ In another study, ⁶⁷Ga-DOTA-GABA-BBN showed less than 1% ID/g uptake in RES organs.³⁴ These studies confirm that small molecule BBN conjugates labeled with Ga-67 or Ga-68 show lower RES organ uptake, when compared with our ⁶⁷Ga labeled BBN-containing AuNPs.

To further evaluate the GRP receptor-targeting efficacy of the radiolabeled nanoconstructs, the uptake of NPs in pancreas, tumor and intestine were analyzed at different post injection time points. It is known in the literature that the GRP receptor density in mice follow the order: pancreas > tumor > intestine, and consequently it is common to observe high uptake in pancreas for BBN derivatives.^{1, 55} At 24h post injection (p.i.) the pancreas uptakes for **NP3-⁶⁷Ga** and **NP4-⁶⁷Ga** were 4.5 and 1.5% ID/g, respectively. Previous studies show that Ga-68-NOTA-BBN conjugate has an uptake of ~5 % ID/g in pancreas within 1 hour of injection and ⁶⁷Ga-DOTA-GABA-BBN derivative showed 1.2% of uptake.^{34, 54} A very high uptake of 27% ID/g was observed in pancreas with ⁶⁸Ga-labeled NOTA-8-Aoc-BBN(7-14)NH₂.⁵⁶ In general, BBN conjugates showed 5 to 20 % ID/g of uptake in GRP receptor over expressing tissues.^{1, 57} When compared with these values, the uptakes observed for our nanoconjugates in pancreas are relatively close to the low range values that have been found in the reported studies. Additional evidence for receptor targeting was obtained by comparing the tumor-uptake data of these conjugates. At 24h p.i, **NP3-⁶⁷Ga** and **NP4-⁶⁷Ga** showed 3.7 and 3.3 %ID/g of radioactivity uptake in tumor, respectively (**Figure 5**). ⁶⁸Ga-NOTA-BBN and ⁶⁷Ga-DOTA-GABA-BBN conjugates reported in literature showed more than 8% and 1.2% ID/g in tumor, respectively.^{34, 54} Overall, nanoconstructs **NP3-⁶⁷Ga** and **NP4-⁶⁷Ga** display uptake in tumor, in line with values found from other BBN compounds reported. Although **NP3-⁶⁷Ga** showed a remarkably high cellular internalization compared to **NP4-⁶⁷Ga** that did not translate to the biodistribution profile. At this point we had questioned whether it was EPR or receptor mediated uptake mechanisms that were predominant for these nanoparticles. In order to answer this, further studies were performed and described as follow.

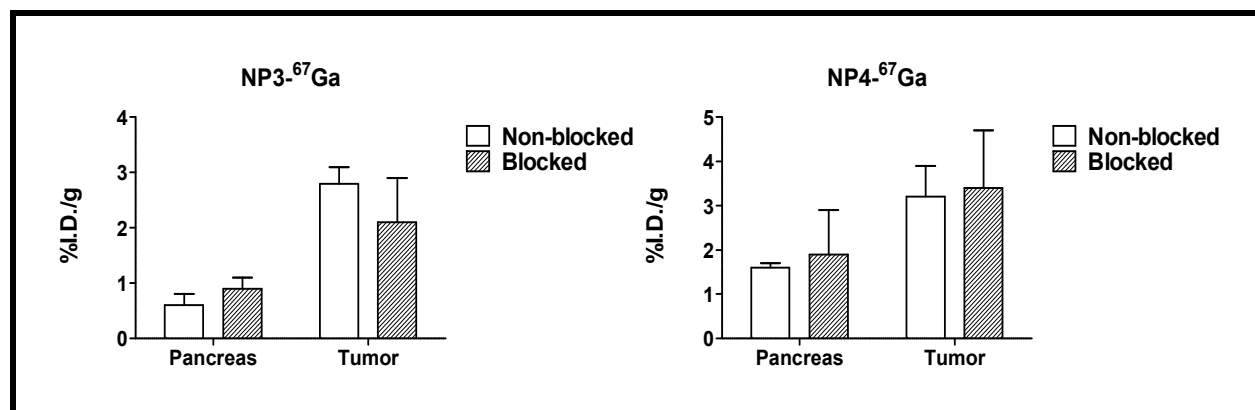


Figure 6. Uptake of NP3-⁶⁷Ga and NP4-⁶⁷Ga in tumor and pancreas with and without blocking by bombesin in BALB/c nude mice bearing human prostate PC3 xenografts at 4 h post injection. Error bars represent the mean \pm standard deviation (n=3). Statistical analysis of the data was done with GraphPad Prism and the level of significance was set at 0.05. For Pancreas p=0.5434; for Tumor p=0.5677. Thus values are not significantly different.

Mechanism of Tumor Uptake

To unravel the mechanism of passive versus active tumor targeting by peptide-conjugated nanoparticles, we studied the uptake of nanoparticles in pancreas and tumor in mice after blocking all non-EPR pathways. In our experiment, we blocked receptors in tumors by injecting free BBN in mice 30 minutes prior to administration of nanoconjugates. After 4 hours of administration, mice were sacrificed and the radioactivity measured in pancreas and tumor (**Figure 6**). Our results indicate that blocking of GRP receptors by BBN showed no effect in uptake of nanoconjugates in both these organs. Between both nanoconstructs, NP3-⁶⁷Ga showed a decrease of $\sim 1\%$ ID/g after blocking with BBN. The results suggest following important conclusions: (i) BBN peptide conjugated nanoparticles are not utilizing receptor mediated pathway as the primary route for targeting tumor; or (ii) EPR pathway is dominant in uptake of NPs in tumor. In addition to the above, the removal of nanoparticles by RES organs also plays a decisive role because the amount of nanoparticles accessible to tumor is largely limited.³ The protein binding characteristics of nanoconjugates may also possibly decide the *in vivo* tumor

uptake. Several reports have already suggested that the biomolecular corona around nanoparticles play important role in deciding the *in vivo* fate of the nanoparticle.^{9, 58} Protein corona becomes very relevant in nanoconjugates that are not functionalized with PEG on the surface, as PEG molecules prevent corona effects.⁵⁹ In fact, preformed albumin corona has been utilized as protective coating for delivery of nanoparticles.⁶⁰ Dawson and coworkers have recently shown that protein corona can significantly alter the targeting characteristics of nanoparticles.^{61, 62} In summary, even though targeting by bombesin nanoconjugates was achieved *in vitro*, the *in vivo* targeting efficacy was dampened possibly due to the exposure of nanoconstructs to complex biochemical milieu.

BBN Nanoconjugates recognize GRP receptor *in vivo*

To evaluate whether the route of administration of nanoparticles in mice have any effect in minimizing protein corona formation which in turn would increase tumor uptake, we chose to administer the conjugate through intraperitoneal (IP) route to mice. IP administrations of nanoconjugates provide immediate access due to proximity of injection site to GRP receptors present in pancreas. IP administration route limits the exposure of nanoconjugates to *in vivo* milieu and decrease the protein corona formation. Previous studies have shown that exposure time of nanoparticles to serum protein is also an important factor in protein corona formation.⁶¹ Furthermore, IP administration would decrease the RES uptake and increase the accessibility of concentration of nanoparticles to target organs. Therefore, we performed following additional studies: (i) Biodistribution of **NP3-⁶⁷Ga** after IP administration. We have selected **NP3-⁶⁷Ga** due to its augmented *in vitro* cell uptake, stability and tumor uptake; (ii) Biodistribution of **NP2-⁶⁷Ga** after IP administration; (iii) IP injection of **NP3-⁶⁷Ga** after blocking the receptors with bombesin (30 minutes prior to injection of nanoconjugate).

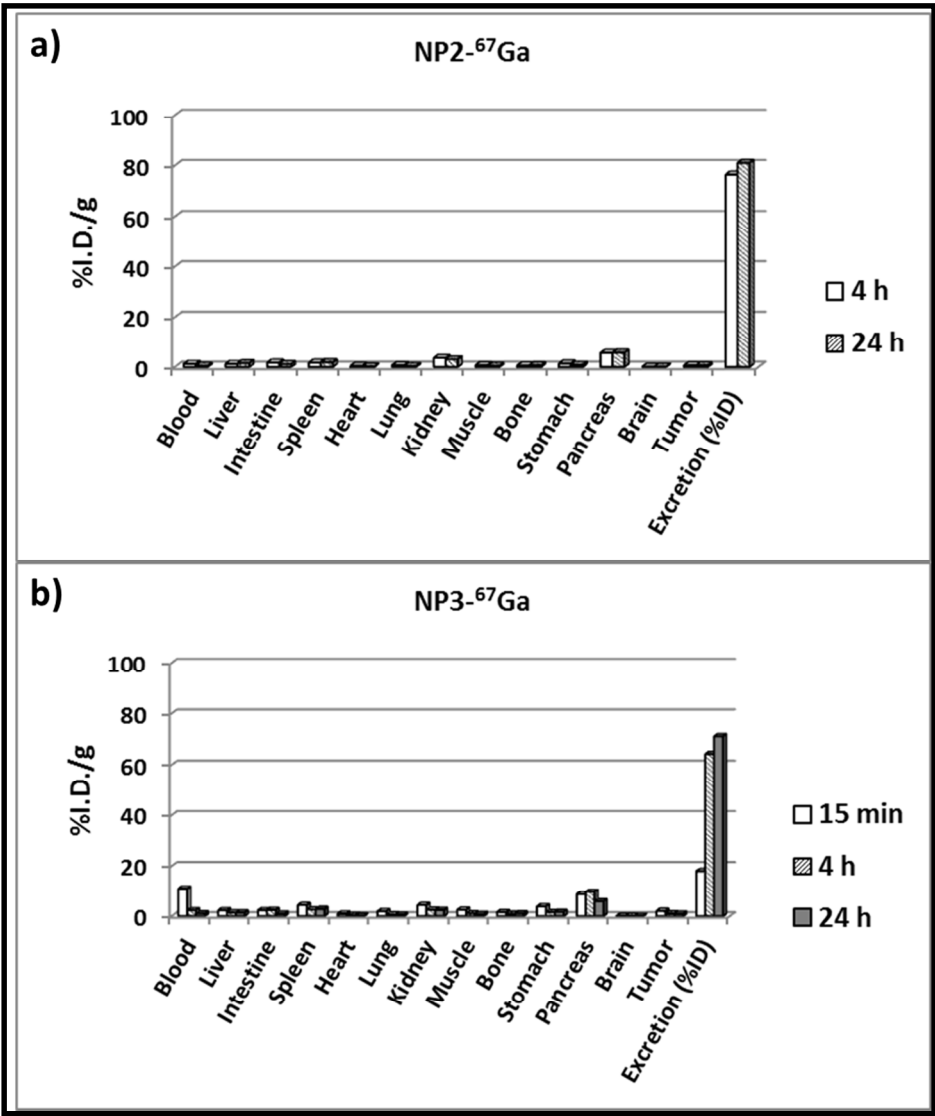


Figure 7. Biodistribution results (mean, n=3; expressed as %I.D./g of organ) for (a) NP2- ^{67}Ga and (b) NP3- ^{67}Ga after i.p. administration in BALB/c nude mice bearing human prostate PC3 xenografts.

The biodistribution profile of NP3- ^{67}Ga after IP injection and IV administrations are different. In particular, the radioactivity uptakes in the liver, spleen and lung are significantly lower, with values $< 5\%$ %ID/g for all the post-injection times. Moreover, there is a significant pancreas uptake of 9.7 ± 1.6 %ID/g at 4 h p.i.. The biodistribution profile of NP2- ^{67}Ga can be considered similar but displayed a lower pancreatic uptake (5.6 ± 0.6 %I.D./g at 4 h p.i.). The tumor uptake for NP3- ^{67}Ga after IP administration is only slightly higher when compared with NP2- ^{67}Ga (0.95

± 0.03 vs 0.65 ± 0.11 %I.D./g at 24 h p.i.) (**Figure 7; ESI-Table 3**). Also the tumor uptake is lower than that exhibited by the same nanoconjugates following IV administration (3.7 ± 0.5 % I.D./g at 24 h p.i.). Altogether, the study showed that there is a slightly increase in uptake of **NP3-⁶⁷Ga** in pancreas. To understand whether this slight increase is receptor mediated, we performed the receptor blocking experiment. In this experiment, BBN peptide was injected IV, 30 minutes prior to injection of **NP3-⁶⁷Ga** through IP. As shown in **Figure 8**, there is a decrease ($\approx 34\%$) of the pancreas uptake of **NP3-⁶⁷Ga**, when blocked with BBN. The result is in accordance with previously reported receptor saturating experiments utilizing antibody labeled nanoparticles. For example, Cai and coworkers have demonstrated that antibody conjugated radiolabeled silica nanoparticles showed a ~ 30 - 40% decrease in tumor uptake upon saturating the receptors with free antibody.⁶³ These results suggest that uptake of **NP3-⁶⁷Ga** in pancreas is possibly being mediated by GRP receptors, but other factors play crucial role in tumor uptake. Nanoconjugates need to travel a longer distance to reach tumor and would meanwhile encounter with large number of serum proteins. This is most likely the reason why the IP administration leads to a lower tumor uptake in comparison to IV administration.

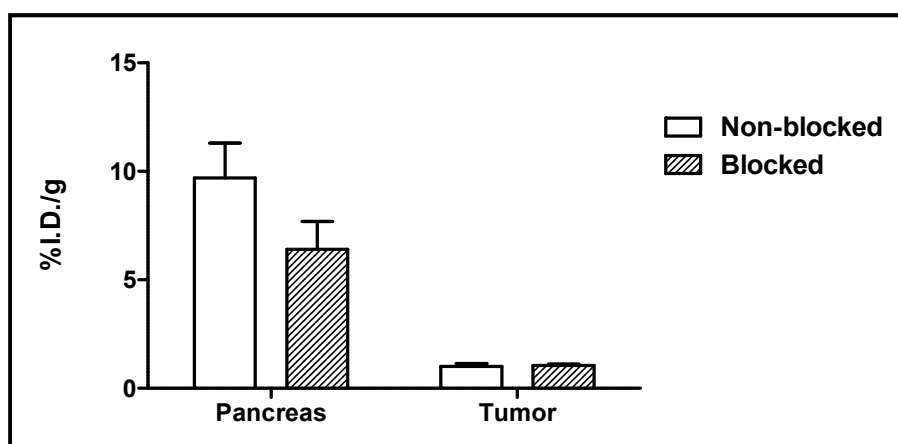


Figure 8. Comparison of the pancreas and tumor uptake (mean \pm SD, $n=2$; expressed as %I.D./g of organ) for **NP3-⁶⁷Ga** after i.p. administration in BALB/c nude mice bearing human prostate PC3 xenografts, treated (blocked) or non-treated with BBN, at 4 h p.i.

CONCLUSIONS

Our initial work was focused on studying the ^{67}Ga -coordination capability of two distinct AuNPs platforms, one stabilized with a DTPA derivative (**NP1**) and another with a DOTA derivative (**NP2**). Nanoconstruct **NP1** lack adequate capacity to maintain optimal Ga-67 coordination in the presence of biological media and apo-transferrin. On the other hand, **NP2** showed moderate to high stability, indicating that DOTA-containing AuNPs were optimal for Ga-67 delivery, and hence, were chosen for BBN-conjugation (**NP3** and **NP4**).

Previous studies in the literature have resulted in conflicting conclusions on the tumor targeting mechanism of nanoparticles, and the factors that govern targeting property of nanoparticles are poorly understood. Nanoconstruct **NP3- ^{67}Ga** displays a remarkably higher cellular internalization compared with **NP4- ^{67}Ga** . However, this did not translate to the biological profile, as it was observed that both nanoconjugates have a similar tumor uptake. We decided to investigate the mechanism of these targeted nanoparticles and performed blocking experiments, wherein the receptors were blocked by free peptide prior to administration of the BBN-conjugated AuNPs. No difference in tumor uptake was observed. These results suggest that active targeting mechanism is not playing a key role. Therefore, we believe that other factors, such as EPR and protein corona influence the transport mechanism of targeted AuNPs to reach tumor. Aiming to obtain further understanding on whether the BBN-conjugated AuNPs recognize receptors *in vivo*, we performed experiments in which the nanoparticles were injected close to organs, other than tumor, that express receptors for bombesin peptide. It is very well known that pancreas in mice overexpress GRP receptors, and therefore we administered **NP3- ^{67}Ga** through IP route. IP injection provided AuNPs in a close proximity to the receptors present in pancreas.

Our results suggest that **NP3- ^{67}Ga** interaction seems to occur with the GRP receptors in pancreas. These nanoconstructs showed up to 3% ID/g more in pancreas compared with non-targeted ones

(NP2-⁶⁷Ga). To further probe on this hypothesis, we blocked the receptors with free bombesin. Here we observed a decrease of ~2.5 to 3% in NP3-⁶⁷Ga uptake in tumor. Taken together, it appears that active targeting plays a role – BBN nanoconjugates target GRP receptors in pancreas, and BBN nanoconjugates showed more uptakes in tumor than non-targeted nanoparticles. On the other hand, receptor blocking experiments reveal that uptake of the BBN-conjugated AuNPs in tumor is mediated by passive mechanism. The contribution of both the mechanism operates in targeting of the AuNPs to tumor. However, the results pointed out that the BBN-conjugated AuNPs are not utilizing the receptor-mediated pathway as the primary route for targeting tumor, playing most probably the EPR pathway a predominant role. In the case of IP administration, the nanoconjugates travel a longer distance to reach tumor than to reach intra peritoneal or retroperitoneal organs. Hence, they have a better chance of getting involved in interactions with circulating serum proteins during their way to the tumor sites, which may cause the corona effect. In brief, it is our reasoning that the receptor mediated pathway *in vivo* is outweighed by the passive EPR effect, or even hindered due to the possible formation of a protein corona enveloping the nanoparticles. In summary, both active and passive targeting play a role in governing the final *in vivo* fate of peptide conjugated nanoparticles. However, it is our reasoning that the significance of these mechanisms is highly dependent on the nanoparticle structure and its physico-chemical properties. Our results encourage further evaluation of these nanoconstructs, considering their proven suitability to retain a stable coordination of ⁶⁷Ga³⁺ under a biological milieu. We anticipate that such suitability will also apply for other medically relevant trivalent radiometals, such as ¹¹¹In, ⁹⁰Y or ¹⁷⁷Lu just to cite a few, conferring a high potential to this newly synthesized AuNPs in the design of multimodal tools for cancer theranostics. To fully explore this possibility, still is crucial to provide the nanoparticle structure with the means to overcome its inability to optimally reach the desired target tumor with adequate payload.

EXPERIMENTAL PROCEDURES

All details of materials and methods including experimental procedures are provided in the supplementary data.

Supporting Information

Supporting Information is available on the ACS Publication website.

ACKNOWLEDGEMENTS

RK thanks Coulter Foundation for providing financial support. Fundação para a Ciência e Tecnologia (FCT) is acknowledged for financial support (EXCL/QEQ-MED/0233/2012). C²TN/IST authors gratefully acknowledge the FCT support through the UID/Multi/04349/2013 project and COST Action TD1004. C. Fernandes is acknowledged for the ESI-MS analyses which were run on a QITMS instrument acquired with the support of the Programa Nacional de Reequipamento Científico (Contract REDE/1503/REM/2005 - ITN) of FCT and is part of RNEM - Rede Nacional de Espectrometria de Massa. A. M. Ferraria would like to thank Prof. A. M. Botelho do Rego for the discussion of XPS results and, also FCT for financial support of PEst-OE/CTM/LA0024/2013. F. Silva thanks FCT for the doctoral research grant (SFRH/BD/47308/2008).

REFERENCES

- (1) Chanda, N., Kattumuri, V., Shukla, R., Zambre, A., Katti, K., Upendran, A., Kulkarni, R. R., Kan, P., Fent, G. M., Casteel, S. W., et al. (2010) Bombesin functionalized gold nanoparticles show in vitro and in vivo cancer receptor specificity. *Proc Natl Acad Sci U S A* 107, 8760-5.
- (2) Chanda, N., Shukla, R., Katti, K. V., and Kannan, R. (2009) Gastrin releasing protein receptor specific gold nanorods: breast and prostate tumor avid nanovectors for molecular imaging. *Nano Lett* 9, 1798-805.
- (3) Brannon-Peppas, L., and Blanchette, J. O. (2004) Nanoparticle and targeted systems for cancer therapy. *Adv Drug Deliv Rev* 56, 1649-59.
- (4) Dreaden, E. C., Mackey, M. A., Huang, X. H., Kang, B., and El-Sayed, M. A. (2011) Beating cancer in multiple ways using nanogold. *Chem Soc Rev* 40, 3391-3404.
- (5) Peer, D., Karp, J. M., Hong, S., Farokhzad, O. C., Margalit, R., and Langer, R. (2007) Nanocarriers as an emerging platform for cancer therapy. *Nature Nanotechnology* 2, 751-760.
- (6) Master, A. M., and Sen Gupta, A. (2012) EGF receptor-targeted nanocarriers for enhanced cancer treatment. *Nanomedicine (Lond)* 7, 1895-906.
- (7) Kudgus, R. A., Walden, C. A., McGovern, R. M., Reid, J. M., Robertson, J. D., and Mukherjee, P. (2014) Tuning pharmacokinetics and biodistribution of a targeted drug delivery system through incorporation of a passive targeting component. *Sci Rep* 4, 5669.
- (8) Bhattacharyya, S., Bhattacharya, R., Curley, S., McNiven, M. A., and Mukherjee, P. (2010) Nanoconjugation modulates the trafficking and mechanism of antibody induced receptor endocytosis. *Proc Natl Acad Sci U S A* 107, 14541-6.
- (9) Huang, X., Peng, X., Wang, Y., Wang, Y., Shin, D. M., El-Sayed, M. A., and Nie, S. (2010) A reexamination of active and passive tumor targeting by using rod-shaped gold nanocrystals and covalently conjugated peptide ligands. *ACS Nano* 4, 5887-96.
- (10) Dreaden, E. C., Austin, L. A., Mackey, M. A., and El-Sayed, M. A. (2012) Size matters: gold nanoparticles in targeted cancer drug delivery. *Ther Deliv* 3, 457-78.
- (11) Hirn, S., Semmler-Behnke, M., Schleh, C., Wenk, A., Lipka, J., Schaffler, M., Takenaka, S., Moller, W., Schmid, G., Simon, U., et al. (2011) Particle size-dependent and surface charge-dependent biodistribution of gold nanoparticles after intravenous administration. *Eur J Pharm Biopharm* 77, 407-16.
- (12) Verma, A., and Stellacci, F. (2010) Effect of Surface Properties on Nanoparticle-Cell Interactions. *Small* 6, 12-21.
- (13) Arvizo, R. R., Miranda, O. R., Moyano, D. F., Walden, C. A., Giri, K., Bhattacharya, R., Robertson, J. D., Rotello, V. M., Reid, J. M., and Mukherjee, P. (2011) Modulating pharmacokinetics, tumor uptake and biodistribution by engineered nanoparticles. *PLoS One* 6, e24374.
- (14) Arvizo, R. R., Miranda, O. R., Thompson, M. A., Pabelick, C. M., Bhattacharya, R., Robertson, J. D., Rotello, V. M., Prakash, Y. S., and Mukherjee, P. (2010) Effect of nanoparticle surface charge at the plasma membrane and beyond. *Nano Lett* 10, 2543-8.
- (15) Khan, J. A., Kudgus, R. A., Szabolcs, A., Dutta, S., Wang, E., Cao, S., Curran, G. L., Shah, V., Curley, S., Mukhopadhyay, D., et al. (2011) Designing nanoconjugates to effectively target pancreatic cancer cells in vitro and in vivo. *PLoS One* 6, e20347.

- (16) Aggarwal, P., Hall, J. B., McLeland, C. B., Dobrovolskaia, M. A., and McNeil, S. E. (2009) Nanoparticle interaction with plasma proteins as it relates to particle biodistribution, biocompatibility and therapeutic efficacy. *Adv Drug Deliv Rev* 61, 428-37.
- (17) Wolfram, J., Yang, Y., Shen, J., Moten, A., Chen, C., Shen, H., Ferrari, M., and Zhao, Y. (2014) The nano-plasma interface: Implications of the protein corona. *Colloids Surf B Biointerfaces* 124, 17-24.
- (18) Wang, Y., Liu, Y., Luehmann, H., Xia, X., Brown, P., Jarreau, C., Welch, M., and Xia, Y. (2012) Evaluating the pharmacokinetics and in vivo cancer targeting capability of Au nanocages by positron emission tomography imaging. *ACS Nano* 6, 5880-8.
- (19) Perrault, S. D., Walkey, C., Jennings, T., Fischer, H. C., and Chan, W. C. (2009) Mediating tumor targeting efficiency of nanoparticles through design. *Nano Lett* 9, 1909-15.
- (20) Perrault, S. D., and Chan, W. C. (2010) In vivo assembly of nanoparticle components to improve targeted cancer imaging. *Proc Natl Acad Sci U S A* 107, 11194-9.
- (21) Kodiha, M., Wang, Y. M., Hutter, E., Maysinger, D., and Stochaj, U. (2015) Off to the organelles - killing cancer cells with targeted gold nanoparticles. *Theranostics* 5, 357-70.
- (22) Zhou, J., and Rossi, J. J. (2014) Cell-type-specific, Aptamer-functionalized Agents for Targeted Disease Therapy. *Mol Ther Nucleic Acids* 3, e169.
- (23) Ding, Y., Jiang, Z., Saha, K., Kim, C. S., Kim, S. T., Landis, R. F., and Rotello, V. M. (2014) Gold nanoparticles for nucleic acid delivery. *Mol Ther* 22, 1075-83.
- (24) Rana, S., Bajaj, A., Mout, R., and Rotello, V. M. (2012) Monolayer coated gold nanoparticles for delivery applications. *Adv Drug Deliv Rev* 64, 200-16.
- (25) Bhattacharyya, S., Singh, R. D., Pagano, R., Robertson, J. D., Bhattacharya, R., and Mukherjee, P. (2012) Switching the targeting pathways of a therapeutic antibody by nanodesign. *Angew Chem Int Ed Engl* 51, 1563-7.
- (26) Kirpotin, D. B., Drummond, D. C., Shao, Y., Shalaby, M. R., Hong, K., Nielsen, U. B., Marks, J. D., Benz, C. C., and Park, J. W. (2006) Antibody targeting of long-circulating lipidic nanoparticles does not increase tumor localization but does increase internalization in animal models. *Cancer Res* 66, 6732-40.
- (27) Bartlett, D. W., Su, H., Hildebrandt, I. J., Weber, W. A., and Davis, M. E. (2007) Impact of tumor-specific targeting on the biodistribution and efficacy of siRNA nanoparticles measured by multimodality in vivo imaging. *Proc Natl Acad Sci U S A* 104, 15549-54.
- (28) Maina, T., Nock, B., and Mather, S. (2006) Targeting prostate cancer with radiolabelled bombesins. *Cancer Imaging* 6, 153-7.
- (29) Abd-Elgalil, W. R., Gallazzi, F., Garrison, J. C., Rold, T. L., Sieckman, G. L., Figueroa, S. D., Hoffman, T. J., and Lever, S. Z. (2008) Design, synthesis, and biological evaluation of an antagonist-bombesin analogue as targeting vector. *Bioconjug Chem* 19, 2040-8.
- (30) Biddlecombe, G. B., Rogers, B. E., de Visser, M., Parry, J. J., de Jong, M., Erion, J. L., and Lewis, J. S. (2007) Molecular imaging of gastrin-releasing peptide receptor-positive tumors in mice using ⁶⁴Cu- and ⁸⁶Y-DOTA-(Pro1,Tyr4)-bombesin(1-14). *Bioconjug Chem* 18, 724-30.
- (31) Lin, K. S., Luu, A., Baidoo, K. E., Hashemzadeh-Gargari, H., Chen, M. K., Brenneman, K., Pili, R., Pomper, M., Carducci, M. A., and Wagner, H. N., Jr. (2005) A new high affinity technetium-99m-bombesin analogue with low abdominal accumulation. *Bioconjug Chem* 16, 43-50.

- (32) Banerjee, S. R., and Pomper, M. G. (2013) Clinical applications of Gallium-68. *Appl Radiat Isot* 76, 2-13.
- (33) Suresh, D., Zambre, A., Chanda, N., Hoffman, T. J., Smith, C. J., Robertson, J. D., and Kannan, R. (2014) Bombesin peptide conjugated gold nanocages internalize via clathrin mediated endocytosis. *Bioconjug Chem* 25, 1565-79.
- (34) Shirmardi, S. P., Gandomkar, M., Maragheh, M. G., and Shamsaei, M. (2011) Preclinical evaluation of a new bombesin analog for imaging of gastrin-releasing peptide receptors. *Cancer Biother Radiopharm* 26, 309-16.
- (35) Chen, Q., Ma, Q., Chen, M., Chen, B., Wen, Q., Jia, B., Wang, F., Sun, B., and Gao, S. (2015) An exploratory study on ^{99m}Tc-RGD-BBN peptide scintimammography in the assessment of breast malignant lesions compared to ^{99m}Tc-3P4-RGD2. *PLoS One* 10, e0123401.
- (36) Faintuch, B. L., Teodoro, R., Duatti, A., Muramoto, E., Faintuch, S., and Smith, C. J. (2008) Radiolabeled bombesin analogs for prostate cancer diagnosis: preclinical studies. *Nucl Med Biol* 35, 401-11.
- (37) Sano, K., Okada, M., Hisada, H., Shimokawa, K., Saji, H., Maeda, M., and Mukai, T. (2013) In vivo evaluation of a radiogallium-labeled bifunctional radiopharmaceutical, Ga-DOTA-MN2, for hypoxic tumor imaging. *Biol Pharm Bull* 36, 602-8.
- (38) Hnatowich, D. J., Friedman, B., Clancy, B., and Novak, M. (1981) Labeling of preformed liposomes with Ga-67 and Tc-99m by chelation. *J Nucl Med* 22, 810-4.
- (39) Wadas, T. J., Wong, E. H., Weisman, G. R., and Anderson, C. J. (2010) Coordinating radiometals of copper, gallium, indium, yttrium, and zirconium for PET and SPECT imaging of disease. *Chem Rev* 110, 2858-902.
- (40) Shanehsazzadeh, S., Oghabian, M. A., Lahooti, A., Abdollahi, M., Haeri, S. A., Amanlou, M., Doha, F. J., and Allen, B. J. (2013) Estimated background doses of [Ga-67]-DTPA-USPIO in normal Balb/c mice as a potential therapeutic agent for liver and spleen cancers. *Nuclear Medicine Communications* 34, 915-925.
- (41) Alric, C., Taleb, J., Le Duc, G., Mandon, C., Billotey, C., Le Meur-Herland, A., Brochard, T., Vocanson, F., Janier, M., Perriat, P., et al. (2008) Gadolinium chelate coated gold nanoparticles as contrast agents for both X-ray computed tomography and magnetic resonance imaging. *Journal of the American Chemical Society* 130, 5908-5915.
- (42) Shan, L. (2004) Gold nanoparticles coated with dithiolated diethylenetriamine pentaacetic acid-gadolinium chelate, in *Molecular Imaging and Contrast Agent Database (MICAD)*, Bethesda (MD).
- (43) Zambre, A., Silva, F., Upendran, A., Afrasiabi, Z., Xin, Y., Paulo, A., and Kannan, R. (2014) Synthesis and characterization of functional multicomponent nanosized gallium chelated gold crystals. *Chem Commun (Camb)* 50, 3281-4.
- (44) Debouttiere, P. J., Roux, S., Vocanson, F., Billotey, C., Beuf, O., Favre-Reguillon, A., Lin, Y., Pellet-Rostaing, S., Lamartine, R., Perriat, P., et al. (2006) Design of gold nanoparticles for magnetic resonance imaging. *Advanced Functional Materials* 16, 2330-2339.
- (45) Brust, M., Walker, M., Bethell, D., Schiffrin, D. J., and Whyman, R. (1994) Synthesis of thiol-derivatized gold nanoparticles in a 2-phase liquid-liquid system. *Journal of the Chemical Society-Chemical Communications*, 801-802.

- (46) Albanese, A., Tang, P. S., and Chan, W. C. W. (2012) The Effect of Nanoparticle Size, Shape, and Surface Chemistry on Biological Systems, in *Annual Review of Biomedical Engineering, Vol 14* (Yarmush, M. L., Ed.) pp 1-16.
- (47) Lindner, S., Michler, C., Wangler, B., Bartenstein, P., Fischer, G., Schirmacher, R., and Wangler, C. (2014) PESIN Multimerization Improves Receptor Avidities and in Vivo Tumor Targeting Properties to GRPR-Overexpressing Tumors. *Bioconjugate Chemistry* 25, 489-500.
- (48) Nam, H. Y., Kwon, S. M., Chung, H., Lee, S. Y., Kwon, S. H., Jeon, H., Kim, Y., Park, J. H., Kim, J., Her, S., et al. (2009) Cellular uptake mechanism and intracellular fate of hydrophobically modified glycol chitosan nanoparticles. *Journal of Controlled Release* 135, 259-267.
- (49) Rejman, J., Oberle, V., Zuhorn, I. S., and Hoekstra, D. (2004) Size-dependent internalization of particles via the pathways of clathrin- and caveolae-mediated endocytosis. *Biochem J* 377, 159-69.
- (50) Oh, N., and Park, J. H. (2014) Endocytosis and exocytosis of nanoparticles in mammalian cells. *Int J Nanomedicine* 9 Suppl 1, 51-63.
- (51) Kannan, R., Rahing, V., Cutler, C., Pandrapragada, R., Katti, K. K., Kattumuri, V., Robertson, J. D., Casteel, S. J., Jurisson, S., Smith, C., et al. (2006) Nanocompatible chemistry toward fabrication of target-specific gold nanoparticles. *J Am Chem Soc* 128, 11342-3.
- (52) Pombo Garcia, K., Zarschler, K., Barbaro, L., Barreto, J. A., O'Malley, W., Spiccia, L., Stephan, H., and Graham, B. (2014) Zwitterionic-coated "stealth" nanoparticles for biomedical applications: recent advances in countering biomolecular corona formation and uptake by the mononuclear phagocyte system. *Small* 10, 2516-29.
- (53) Zhao, Y., Sultan, D., Detering, L., Cho, S., Sun, G., Pierce, R., Wooley, K. L., and Liu, Y. (2014) Copper-64-alloyed gold nanoparticles for cancer imaging: improved radiolabel stability and diagnostic accuracy. *Angew Chem Int Ed Engl* 53, 156-9.
- (54) Varasteh, Z., Velikyan, I., Lindeberg, G., Sorensen, J., Larhed, M., Sandstrom, M., Selvaraju, R. K., Malmberg, J., Tolmachev, V., and Orlova, A. (2013) Synthesis and characterization of a high-affinity NOTA-conjugated bombesin antagonist for GRPR-targeted tumor imaging. *Bioconjug Chem* 24, 1144-53.
- (55) Schuhmacher, J., Zhang, H., Doll, J., Macke, H. R., Matys, R., Hauser, H., Henze, M., Haberkorn, U., and Eisenhut, M. (2005) GRP receptor-targeted PET of a rat pancreas carcinoma xenograft in nude mice with a 68Ga-labeled bombesin(6-14) analog. *J Nucl Med* 46, 691-9.
- (56) Dijkgraaf, I., Franssen, G. M., McBride, W. J., D'Souza, C. A., Laverman, P., Smith, C. J., Goldenberg, D. M., Oyen, W. J., and Boerman, O. C. (2012) PET of tumors expressing gastrin-releasing peptide receptor with an 18F-labeled bombesin analog. *J Nucl Med* 53, 947-52.
- (57) Kannan, R., Pillarsetty, N., Gali, H., Hoffman, T. J., Barnes, C. L., Jurisson, S. S., Smith, C. J., and Volkert, W. A. (2011) Design and synthesis of a bombesin peptide-conjugated tripodal phosphino dithioether ligand topology for the stabilization of the fac-[M(CO)3]+ core (M=(99 m)Tc or Re). *Inorg Chem* 50, 6210-9.
- (58) Sasidharan, A., Riviere, J. E., and Monteiro-Riviere, N. A. (2015) Gold and silver nanoparticle interactions with human proteins: impact and implications in biocorona formation. *J Mater Chem B* 3, 2075-2082.

- (59) Berret, J. F. (2007) Stoichiometry of electrostatic complexes determined by light scattering. *Macromolecules* 40, 4260-4266.
- (60) Peng, Q., Zhang, S., Yang, Q., Zhang, T., Wei, X. Q., Jiang, L., Zhang, C. L., Chen, Q. M., Zhang, Z. R., and Lin, Y. F. (2013) Preformed albumin corona, a protective coating for nanoparticles based drug delivery system. *Biomaterials* 34, 8521-30.
- (61) Salvati, A., Pitek, A. S., Monopoli, M. P., Prapainop, K., Bombelli, F. B., Hristov, D. R., Kelly, P. M., Aberg, C., Mahon, E., and Dawson, K. A. (2013) Transferrin-functionalized nanoparticles lose their targeting capabilities when a biomolecule corona adsorbs on the surface. *Nature Nanotechnology* 8, 137-143.
- (62) Gaspar, R. (2013) Nanoparticles: Pushed off target with proteins. *Nat Nanotechnol* 8, 79-80.
- (63) Chen, F., Hong, H., Shi, S., Goel, S., Valdovinos, H. F., Hernandez, R., Theuer, C. P., Barnhart, T. E., and Cai, W. (2014) Engineering of hollow mesoporous silica nanoparticles for remarkably enhanced tumor active targeting efficacy. *Sci Rep* 4, 5080.

TABLE OF CONTENTS

Interrogating the Role of Receptor-Mediated Mechanisms: Biological Fate of Peptide-functionalized Radiolabeled Gold Nanoparticles in Tumor Mice

Francisco Silva, Ajit Zambre, Maria Paula Cabral Campello, Lurdes Gano, Isabel Santos, Ana Maria Ferraria, Maria João Ferreira, Amolak Singh, Anandhi Upendran, António Paulo and Raghuraman Kannan

